Nanocrystal-enhanced near-IR emission in the bismuth-doped chalcogenide glasses

Yinsheng Xu (许银生)[1,2], **Jiani Qi (戚嘉妮)**[1,2], **Changgui Lin (林常规)**[1,2], **Peiqing Zhang (张培晴)**[2,3], **and Shixun Dai (戴世勋)**[2,3*]

[1]*Faculty of Materials Science and Chemical Engineering, Ningbo University, Ningbo 315211, China*

[2]*Laboratory of Infrared Materials and Devices, Ningbo University, Ningbo 315211, China*

[3]*Faculty of Information Science and Engineering, Ningbo University, Ningbo 315211, China*

Corresponding author: daishixun@nbu.edu.cn

Received October 24, 2012; accepted November 16, 2012; posted online March 6, 2013

Bismuth (Bi)-doped materials have attracted a great deal of attention because of their broadband near-infrared (near-IR) emission around the wavelength utilized in telecommunications. In this study, broad near-IR emission band from 1 100 to 1 650 nm is generated in the Bi-doped $90GeS_2$-$10Ga_2S_3$ glass and glass-ceramics under 820 nm of light excitation. Based on the analysis of the absorption and emission spectra, the origin of this broadband emission is ascribed to the Bi_2^{2-} dimers. The precipitation of β-GeS_2 nanocrystals drastically enhances the emission intensity and lifetime of Bi-doped chalcogenide glass.

OCIS codes: 160.2540, 160.2750, 300.2140.

doi: 10.3788/COL201311.041601.

The development of wavelength division multiplexing (WDM) technology based on Er^{3+} ion-doped fiber amplifier has promoted the progress of optical communication over the past decades. However, Er^{3+} ion-doped optical amplifiers can only generate optical amplification at around 1.55 μm, with a bandwidth of less than 80 nm, because of the limited luminescent bandwidth of $4f$–$4f$ transition. As the transmission capability of the current 1.55-μm window is closely approaching saturation, the amplifiers in the 1.31-μm communication window, where the silica glass fiber shows zero dispersion, has started to draw the attention of researchers. Dy^{3+} and Pr^{3+} ions are the most explored rare-earth (RE) ions because of their 1.31-μm fiber amplifier. However, these ions have limited bandwidth. Thus, researchers started search for host materials with lower phonon energy or multiple RE-ion co-doping technologies to surpass this bandwidth limitation[1−3]. Fujimoto *et al.* pioneered the work on novel infrared (IR) luminescent from Bi-doped silica glasses and generated 1.31-μm optical amplification under 0.8-μm excitation[4]. Meng *et al.* later investigated the Bi luminescence phenomena under different oxide glass compositions[5−8]. Recently, Dianov *et al.* made great progress on the Bi-doped fiber laser[9−11], wherein a 2-W fiber laser has been generated in the wavelength ranging from 1 300 to 1 500 nm. This remarkable progress indicated that Bi-doped materials are the most promising candidates for the fiber amplifier or fiber laser in the NIR range.

Among all kinds of host glasses, chalcogenide glasses exhibit low phonon energy, which can decrease the multiphonon relaxation rate and allow the observation of certain transitions in RE dopants that cannot be observed in traditional glasses such as silica[12]. Ren *et al.* first reported luminescence of Bi-doped chalcohalide glasses; however, the obtained glasses exhibited poor chemical durability because of the large amount of KBr contained[13−15]. In 2008, Dong *et al.* reported the broad emission with 200-nm full-width of half-maximum (FWHM) in chalcogenide glass and suggested that the low valence state of Bi contributed to the broadband IR luminescence[16]. Recently, Hughes *et al.* reported a super broad emission of Bi (FWHM=800 nm) in the gallium lanthanum sulphide (GLS) glass[17]. Therefore, further studying the Bi-doped chalcogenide glass to obtain more evidence to clarify the origin of the broad NIR emission is necessary. The nanocrystal-enhanced NIR emission has been realized in the present work. The extremely low phonon energy and improved mechanical strength of chalcogenide glass-ceramics are favorable properties. The assumption of the origin has been proposed by comparing the absorption and emission spectra of the alumosilicate or GLS glasses[17,18].

The $90GeS_2$-$10Ga_2S_3$ glass was selected as the matrix. The bandgap wavelength of the chalcogenide glass is very sensitive to the Bi contents[16]. Thus, only 0.25-mol% Bi_2S_3 was introduced as dopant to keep the pump laser from not being absorbed by the glass matrix. Ten grams each of highly-pure germanium, gallium, sulfur, and Bi with 5 N purity were mixed and introduced into a fused quartz tube with a 10-mm-inner-diameter. The tube was sealed under vacuum, and then melted in a rocking furnace for over 10 h at 980 °C. The temperature was decreased to 900 °C, and then the silica tube was quenched vertically into water after 2 h. The sample was annealed at 350 °C for 2 h and slowly cooled to room temperature to remove the inner stress. Afterward, the tube was carefully broken and the glass rods were obtained. After cutting and polishing, several slices of the sample with double-mirrored surface were prepared for further heat treatment (HT). A 10-mg sample was used to measure the glass transition temperature (T_g) using the Q2000 differential scanning calorimeter (DSC, TA instrument, New Castle, DE, USA). According to the DSC curve of the Bi-doped GeS_2-Ga_2S_3 glass, the T_g was 366 °C when the heating rate was 10 °C/min. Subsequently, the se-

lected samples were treated at 386 °C ($T_g + 20$ °C) with different durations.

Powder X-ray diffraction (XRD) measurement was performed on a D2 (Bruker Corp., Ettlingen, Germany) diffractometer (Voltage=30 kV, current=10 mA, Cu Ka) with a step width of 0.02° to verify the amorphous state or crystallization of the samples. The XRD patterns of the glasses were collected in the range of $10° < 2\theta < 80°$. A VEGA 3 SBH scanning electron microscope (SEM, Tescan, Brno, Czech Republic) in secondary electron mode was used to observe the interior of the glass ceramic. Optical absorption spectra were measured using the Lambda 950 UV/VIS/NIR spectrophotometer (Perkin-Elmer, Massachusetts, USA) at room temperature. The emission spectra and the fluorescence decay curves were recorded using a FLS920 fluorescence (Edinburgh Instruments Ltd., Livingston, UK) spectrophotometer. The emission spectra were collected by liquid nitrogen-cooled Hamamatsu R5509-72 photomultiplier tubes in the range of 1 000 to 1 700 nm, with a 450-W Xe lamp as the excitation source. An 850-nm filter was placed in front of the detector to eliminate the noise from the excitation lamp. All the emission spectra were corrected by the correction files supplied by the manufacturer.

Figure 1 shows the absorption spectra of the glass sample heat-treated at 386 °C with different durations. Surprisingly, a weak absorption band centered on 820 nm appeared. Hughes *et al.* observed this absorption band around 850 nm[17], but this absorption band was not given any attention. This absorption transition matched well to the Bi_2^{2-} dimers[18] and guaranteed the pumping scheme used in this study. The absorption edge, λ_{vis}, of the glass is very sensitive to the presence of crystal in the glass matrix. With longer heat treatment, a red-shift of the λ_{vis} was observed, indicating that nanocrystals precipitated in the glass matrix. The SEM images also confirmed that the nanocrystals have precipitated in the sample heat treated for 36 h, as shown on the top right portion of Fig. 1. Clearly, the size of the crystals is less than 100 nm, but not homogeneous.

Figure 2 shows the X-ray diffraction of the glass samples heat-treated at 386 °C for 36 h. Compared with that of the precursor glass, several small peaks appeared on the XRD pattern. Another sample was heat-treated at 460 °C for 24 h and prepared as a reference to clearly observed the crystallization peak. The XRD pattern of
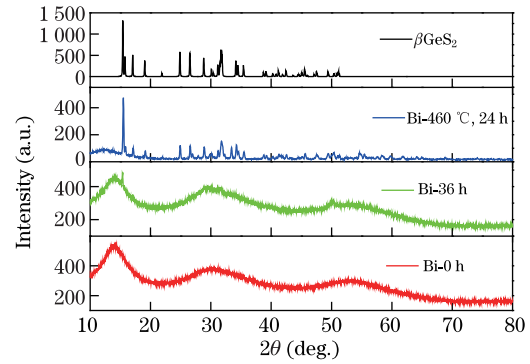
Fig. 2. XRD patterns of the glass samples heat-treated at 386 °C for 0 and 36 h, respectively. The patterns of the sample heat-treated at 460 °C for 24 h and β-GeS_2 are also included as references.

the reference sample is consistent with the β-GeS_2 crystals. This observation is similar to our previous study on (100-x) $GeS_2 - xGa_2S_3$ (mol %) glasses, where the β-GeS_2 precipitated first while the x was less than 14.3 mol %[19]. The average size of the crystals was calculated as 62 nm using the Scherrer equation. The calculated size of the crystals agrees with the observation under SEM. Under the 820-nm light excitation, a broad NIR emission band from 1 100 to 1 650 nm can be observed in Fig. 3. The spectroscopic analysis was limited because of the upper limit of the spectrometer at 1 700 nm. With longer HT, the emission intensity was much enhanced and the FWHM increased from 182 to 204 nm. The emission band of RE ions becomes sharper (or narrower) after the crystallization of the glass because of the crystal field effect. However, the broader FWHM of the Bi ions was probably due to the more luminescent center formed in the glass after heat treatment. This broadband emission covers the O, E, S, C, L bands (1 260 to 1 625 nm), indicating that Bi-doped chalcogenide glass is promising for ultra-broadband amplification. After Gaussian fitting, three emission bands centered 1 273, 1 490, and 1 593 nm was observed. A similar broad emission was found by Hughes *et al.* under 980-nm excitation[17]. Unfortunately, the emission spectrum measured under 808-nm excitation was not shown in his paper, thus we cannot provide more comparisons.

The fluorescence decay curve of the glass sample heat-treated at 386 °C for 36 h and monitored at 1 273 nm is shown in Fig. 4. This decay and the other measured
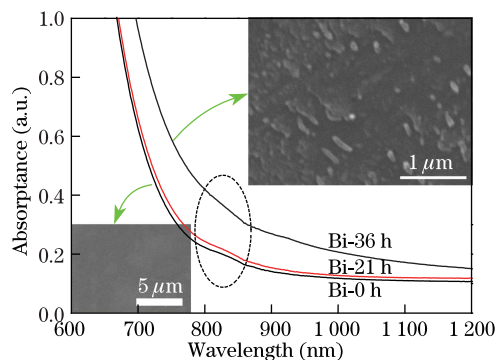

Fig. 1. Absorption spectra of the glass samples heat-treated at 386 °C for 0, 21, and 36 h, respectively. Insets are the corresponding SEM images.
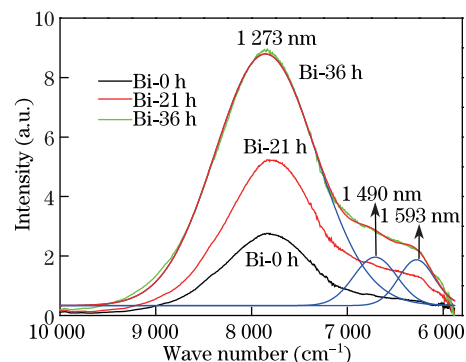

Fig. 3. Emission spectra of the glass samples heat-treated at 386 °C for 0, 21, and 36 h, respectively.
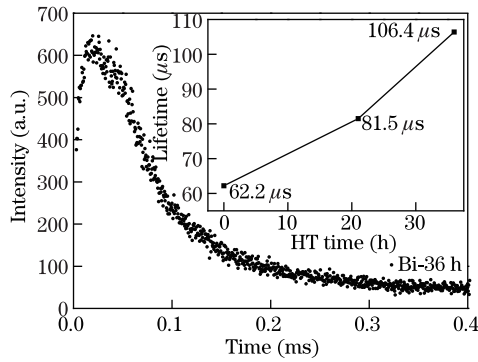
Fig. 4. Time decay curves monitored at 1 275 nm of the glass samples heat-treated at 386 °C for 36 h. Inset: dependence of decay time on the HT durations.

emission decays cannot be fitted well with the first-order exponential decay. However, the second-order exponential decay equation with better-fitting results can be used, indicating that the decay process may consist of one slow process and one fast process. This fluorescence decay deviation is probably due to the Bi ions occupying different sites in the disordered glass matrix. Thus, the mean decay time was used to calculate the fluorescence lifetime using

$$\tau_{\mathrm{m}} = \int_{t_0}^{\infty} \frac{I(t)\mathrm{d}t}{I_0}, \tag{1}$$

where $I(t)$ is the luminescence intensity as a function of time t and I_0 is the maximum of $I(t)$ that occurs at the initial time t_0. With longer HT, the lifetime of the glass samples increased almost linearly from 62.2 to 106.4 μs, as shown in the inset of Figure 4. The emission spectra and the fluorescence decay curve suggested that the β-GeS$_2$ nanocrystals have a positive effect on the NIR emission. The multi-phonon relaxation process usually quenches the radiative transition of transition metal ions. The room temperature luminescent decay time, τ, is mainly determined by the non-radiative decay time, τ_{nr}. According to the Mott and Gurney model, τ_{nr} can be described by a single Arrhenius factor related to the occupation probability of the electrons in the vibration excited state:

$$\tau_{\mathrm{nr}} = A \exp\left(-\frac{\Delta E}{kT}\right), \tag{2}$$

where A is a constant, k is the Boltzmann constant, ΔE is the activation energy, and T is the temperature. According to the single configurational coordinate model, the stronger the crystal field is for a specific site distribution, the larger the activation energy. Therefore, the longer emission lifetime was due to the stronger crystal field caused by the precipitation of β-GeS$_2$ crystals.

However, the exact valent bismuth ion that contributes to the infrared emission still needs to be determined[4]. Some authors insisted on the Bi^{3+} or Bi^{5+} ion, based on the 27Al-NMR, ESR, XPS, and EXAFS measurements; however, Meng et al.[5−7] suggested that the Bi$_n$ clusters or low valence state of Bi (such as Bi$^+$, Bi^{2+})

resulted in the IR luminescence. Dianov et al. performed quantum-chemical calculations on the spectroscopic properties of Bi$_2^-$ and Bi$_2^{2-}$ dimers and proved that the interstitial negative Bi dimers are the centers of the NIR luminescence[18]. Although the aforementioned views were confirmed by various evidence, we cannot provide a conclusion on which valence of Bi is the origin of the NIR luminescence. Cubicciotti studied the reaction between Bi and S, and suggested that the synthetic is Bi$_2$S$_3$[20,21]. When Bi is introduced into the chalcogenide glass, the valence of the Bi ions tends to maintain a low valence state because of the high deoxidization of the sulfur. Considering the absorption peak around 820 nm and the broad NIR emission from 1 100 to 1 650 nm, it is reasonable to exclude the Bi$^+$: ^{3}P$_0 \rightarrow ^3$P$_2$ because a 1 475-nm emission cannot be generated from Bi$^+$ ions. Between the Bi^{2+} ions and Bi$_2^{2-}$ dimers, the emission characteristic of the latter is similar to the present study[18]. Hughes et al.[17] found emission bands at 2 000 to 2 600 nm in the GLS glass at low temperature, and proposed that the emission is ascribed to the transitions $^1\sum_0 \rightarrow ^3\sum_0^+$ and $^1\sum_0^+ \rightarrow ^3\sum_0^+$ of the low-lying states of a Bi$_2^{2-}$ dimers. Therefore the Bi$_2^{2-}$ dimers is the most probable reason for the broadband near-IR emission.

In conclusion, broad NIR emission extending from 1 100 to 1 650 nm is generated in the Bi-doped 90GeS$_2$-10Ga$_2$S$_3$ glass. The origin of this broad emission is probably related to the Bi$_2^{2-}$ dimers. The precipitation of the β-GeS$_2$ nanocrystals enhanced the emission intensity and the lifetime of Bi$_2^{2-}$ dimers. These observations show that the Bi-doped chalcogenide glass ceramic would be a new active medium for NIR lasers and amplifiers.

References

1. V. K. Tikhomirov, K. Driesen, C. Göller-Walrand, and M. Mortier, Opt. Express **15,** 9535 (2007).
2. D. Chen, Y. Wang, F. Bao, and Y. Yu, J. Appl. Phys. **101,** 113511 (2007).
3. Y. Xu, D. Chen, W. Wang, Q. Zhang, H. Zeng, C. Shen, and G. Chen, Opt. Lett. **33,** 2293 (2008).
4. Y. Fujimoto and M. Nakatsuka, Jpn. J. Appl. Phys. **40,** L279 (2001).
5. X. Meng, J. Qiu, M. Peng, D. Chen, Q. Zhao, X. Jiang, and C. Zhu, Opt. Express **13,** 1628 (2005).
6. M. Peng, J. Qiu, D. Chen, X. Meng, and C. Zhu, Opt. Express **13,** 6892 (2005).
7. M. Peng, B. Wu, N. Da, C. Wang, D. Chen, C. Zhu, and J. Qiu, J. Non-Cryst. Solids **354,** 1221 (2008).
8. M. Peng, X. Meng, J. Qiu, Q. Zhao, and C. Zhu, Chem. Phys. Lett. **403,** 410 (2005).
9. E. M. Dianov, S. V. Firstov, V. F. Khopin, O. I. Medvedkov, A. N. Guryanov, and I. A. Bufetov, Quantum Electron. **39,** 299 (2009).
10. E. M. Dianov, J. Non-Cryst. Solids **355,** 1861 (2009).

11. S. V. Firstov, I. A. Bufetov, V. F. Khopin, A. V. Shubin, A. M. Smirnov, L. D. Iskhakova, N. N. Vechkanov, A. N. Guryanov, and E. M. Dianov, Laser Phys. Lett. **6,** 665 (2009).

12. Y. Xu, D. Chen, Q. Zhang, H. Zeng, C. Shen, J.-L. Adam, X. Zhang, and G. Chen, J. Phys. Chem. C **113,** 9911 (2009).

13. G. Yang, D. Chen, W. Wang, Y. Xu, H. Zeng, Y. Yang, and G. Chen, J. Eur. Ceram. Soc. **28,** 3189 (2008).

14. J. Ren, D. Chen, G. Yang, Y. Xu, H. Zeng, and G. Chen, Chin. Phys. Lett. **24,** 1958 (2007).

15. G. Yang, D. Chen, J. Ren, Y. Xu, H. Zeng, Y. Yang, and

16. G. Chen, J. Am. Ceram. Soc. **90,** 3670 (2007).

16. G. Dong, X. Xiao, J. Ren, J. Ruan, X. Liu, J. Qiu, C. Lin, H. Tao, and X. Zhao, Chin. Phys. Lett. **25,** 1891 (2008).

17. M. A. Hughes, T. Akada, T. Suzuki, Y. Ohishi, and D. W. Hewak, Opt. Express **17,** 19345 (2009).

18. V. O. Sokolov, V. G. Plotnichenko, and E. M. Dianov, Opt. Lett. **33,** 1488 (2008).

19. C. Lin, L. Calvez, H. Tao, M. Allix, A. Moréc, X. Zhang, and X. Zhao, J. Solid State Chem. **184,** 584 (2011).

20. D. Cubicciotti, J. Phys. Chem. **66,** 1205 (1962).

21. D. Cubicciotti, J. Phys. Chem. **67,** 1385 (1963).